

RESEARCH

Open Access



Pathogenesis of human atheroma necrotic core: degradation of connective tissue fibers and possible involvement of cathepsin K

Kazunori Nakagawa¹ and Yutaka Nakashima^{1*} 

Abstract

Background Atheroma is a serious atherosclerotic lesion related to plaque rupture, thrombosis, and ischemic disease. To clarify the pathogenesis of human atheroma, particularly the formation of the liponecrotic tissue in the necrotic core, the distribution of connective tissue fibers, such as collagen and elastic fibers, and related substances was investigated in this study.

Methods Atherosclerotic lesions in human coronary arteries were classified into three categories: pathologic intimal thickening (PIT), atheroma with lipid core (ALC), and atheroma with necrotic core (ANC). PIT and ALC consisted of the lipid pool and the lipid core, respectively. The necrotic core of ANC was composed of a lipid core-like region and liponecrotic tissue containing amorphous materials and lacking cells and connective tissue fibers. The distribution of collagen type I, elastin, C-terminal crosslinked telopeptide of collagen type I (CTX-I), and cathepsin K (CatK) was investigated through immunohistochemistry. CTX-I is a fragmented peptide consisting of the C-terminal region of collagen type I that is generated by CatK. The distribution of denatured and unfolded collagen chains was also investigated through collagen hybridizing peptide staining.

Results Collagen type I, denatured and unfolded collagen chains, and elastin were positively stained in the PIT, ALC, and lipid core-like region of ANC. However, they were negatively stained in the liponecrotic tissue of ANC. CTX-I and CatK were positively stained in all four regions, and their grade of staining appeared to show a positive relationship. Both CTX-I and CatK demonstrated higher staining grades in the liponecrotic tissue. These findings suggested that pre-existing collagen type I was severely degraded by CatK, resulting in the production of CTX-I in the liponecrotic tissue, and that pre-existing elastin was also degraded in this region. CatK was mainly found in macrophage foam cells, many of which were localized within and around the liponecrotic tissue.

Conclusions This study suggests that the liponecrotic tissue in the necrotic core of human atheroma is formed by severe degradation of pre-existing connective tissue fibers and consequent collapse of tissue structure. This degradation is likely caused by proteolytic enzymes, such as CatK, secreted by macrophage foam cells.

Keywords Human, Atheroma, Necrotic core, Liponecrotic tissue, Collagen type I, CTX-I, Cathepsin K, Macrophage foam cells

*Correspondence:

Yutaka Nakashima
yutaka-nakashima@kyudai.jp

¹ Pathophysiological and Experimental Pathology, Graduate School of Medical Sciences, Kyushu University, 3-1-1 Maidashi, Higashi-Ku, Fukuoka 812-8582, Japan

Background

According to the World Health Organization (WHO), cardiovascular diseases (CVDs) are the leading cause of death worldwide [1]. CVDs caused approximately 18 million deaths in 2019, with 85% of them caused by heart attack and stroke [1]. Often, the heart attacks are



© The Author(s) 2024. **Open Access** This article is licensed under a Creative Commons Attribution-NonCommercial-NoDerivatives 4.0 International License, which permits any non-commercial use, sharing, distribution and reproduction in any medium or format, as long as you give appropriate credit to the original author(s) and the source, provide a link to the Creative Commons licence, and indicate if you modified the licensed material. You do not have permission under this licence to share adapted material derived from this article or parts of it. The images or other third party material in this article are included in the article's Creative Commons licence, unless indicated otherwise in a credit line to the material. If material is not included in the article's Creative Commons licence and your intended use is not permitted by statutory regulation or exceeds the permitted use, you will need to obtain permission directly from the copyright holder. To view a copy of this licence, visit <http://creativecommons.org/licenses/by-nc-nd/4.0/>.

caused by obstruction of coronary arteries, resulting in ischemic heart disease (IHD) [1]. As atherosclerosis is a major contributor to the obstruction, it is crucial to better understand its pathogenesis to prevent and treat IHD. Currently, many research efforts are focused on the etiology and development of atherosclerosis in humans [2–9], with experimental studies also being performed in animal models [10–13]. Animal models are very useful to clarify certain features of the pathology of atherosclerosis, such as asymptomatic lesion development and the role of atherogenic proteins and cells. However, animal models are less helpful for investigating the complications of atherosclerosis, such as rupture of the plaque core and subsequent thrombosis [14, 15]. This limitation suggests that the mechanism of atherosclerosis, particularly that of plaque rupture, should be thoroughly investigated using human materials. Atherosclerosis in humans progresses from early lesions to pathologic intimal thickening (PIT) and then to advanced lesions. PIT is an intermediate lesion consisting of a lipid pool [2, 8, 16], and advanced lesions include atheromas, fibrous plaque, and calcified lesion [3, 4]. Atheromas carry a risk for plaque rupture, and other lesions are largely asymptomatic unless they cause severe luminal stenosis. Thus, atheromas can be seen as the pathological manifestations of the disease known as atherosclerosis. Atheromas are lesions commonly found in coronary arteries in adults. Previously, we investigated risk factors for coronary atherosclerosis using autopsy patients from the general population [17]. During the histological investigation, we found that about 70% of autopsied patients over 40 years of age had one or more atheroma lesions in major coronary arteries.

It is generally believed that the core of the atheroma develops through the accumulation of intracytoplasmic lipids and cellular debris released from dead macrophage foam cells. The rationale is that apoptotic and necrotic macrophages are present in advanced lesions [9, 18], but the pathogenic mechanism of human atheroma remains to be fully clarified. In our previous study using coronary arteries of autopsy patients and imaging mass spectrometry analysis, the following three mechanisms were proposed for the pathogenesis of human atheroma [9]: (1) human atheroma develops mainly through the infiltration and deposition of plasma lipids; (2) liponecrotic tissue in the necrotic core of atheroma develops through the loss of pre-existing connective tissue fibers; (3) macrophages play an important role in the loss of connective tissue fibers. These hypotheses were derived from four major observations and suggestions in the study [9]. First, we demonstrated that human atheromas can be classified into two categories: atheroma with a lipid core (ALC) and atheroma with a necrotic core (ANC) [9]. The necrotic core consisted of a lipid core-like region and liponecrotic

tissue. Second, the study suggested that a major portion of the lipids was derived from the plasma in ALC and ANC [9]. Third, connective tissue fibers were absent in the liponecrotic tissue of ANC [9]. Fourth, macrophage foam cells accumulated around the liponecrotic tissue [9].

Therefore, in this study, we aimed to clarify the pathogenesis of human atheroma, focusing, in particular, on the degradation and loss of connective tissue fibers, that is, collagen and elastic fibers, because it was hypothesized that connective tissue fibers were degraded in the liponecrotic tissue by proteolytic enzymes. For this purpose, the distribution of collagen type I, collagen type III, elastin, denatured and unfolded collagen chains, C-terminal crosslinked telopeptide of collagen type I (CTX-I), and cathepsin K (CatK) was immunohistochemically and histologically investigated in PIT, ALC, and ANC. Collagen type I, collagen type III, and elastin are the major components of connective tissue fibers in atherosclerotic lesions [19–21]. Denatured and unfolded collagen chains are detected using collagen hybridizing peptide (CHP) staining [22, 23]. CTX-I is a degradation product of collagen type I [24, 25], and CatK is a potent collagenolytic and elastinolytic cysteine protease [26, 27]. Based on the staining results for these six substances, this study proposes a novel mechanism for the pathogenesis of atheroma in humans.

Methods

Autopsy patients and classification of atherosclerotic lesions

The proximal segments of the left anterior descending artery (LAD) and the right coronary artery (RCA) obtained from 16 Japanese autopsy patients were used in this study. The patients included some of the patients used in a previous study [9]. The principal diseases of the patients are presented in Additional Table 1 [see Additional file 1]. There was no significant difference from the types of diseases observed in the Japanese population. We collected coronary artery specimens randomly from the autopsy patients, and no IHD was found in any patient. Cerebral infarction was found in three older patients (aged 85, 89, and 93 years old, respectively) and the grade of their coronary atherosclerosis was relatively severe, with ALC in one patient and ANC in two patients. A history of diabetes mellitus was reported in a 61-year-old patient who died of esophageal cancer and showed a mild grade of coronary atherosclerosis (PIT). Table 1 summarizes the clinical and laboratory data, which were not largely different from those in the general population. No patient was found to be obese, using the Japanese criteria of a body mass index of 25 kg/m² or over [28]. A serum glucose

Table 1 Characteristics of the autopsy patients

	<i>n</i> ^c	mean ± SD ^d	range	number
Age (years)	16	73.3 ± 12.9	51–93	
Gender (M/F) ^a	16			10/6
Smoking status (S/NS/UNK) ^b	16			10/4/2
Body mass index (kg/m ²)	15	19.8 ± 3.6	13.7–24.7	
Serum glucose (mg/dL)	11	100.6 ± 35.9	55–176	
Serum total cholesterol (mg/dL)	15	166.5 ± 46.8	97–239	
Systolic blood pressure (mmHg)	13	125.5 ± 15.0	104–155	
Diastolic blood pressure (mmHg)	13	76.8 ± 10.6	60–92	

^a M male, F female^b S smoker, NS non-smoker, UNK unknown^c *n* number of patients^d SD standard deviation

level of over 100 mg/dL was found in five patients. The coronary atherosclerosis grade in these patients was found to be skewed neither towards mild or severe lesions, with PIT in three patients, ALC in one patient, and ANC in one patient. No patient had serum total cholesterol level over 240 mg/dL.

The atherosclerotic lesions were divided into three groups: PIT, ALC, and ANC, as previously described [9]. PIT is defined as a lesion consisting of lipid pools with mild macrophage infiltration [2, 8, 29]. The lipid pools are characterized by a mild accumulation of extracellular lipids that is generally ill-defined [2, 8]. In this study, the area with extracellular lipid deposits was lightly stained with hematoxylin and eosin (H & E), elastica van Gieson (EVG), and picosirius red (PSR) staining, and positively immunostained for apolipoprotein B (apoB). Smooth muscle cells (SMCs) and elastic and collagen fibers were discretely distributed in the lipid pool.

ALC is defined as a lesion with the accumulation of a large amount of extracellular lipids in the intima to form a well-defined lipid core [3, 9]. Varying numbers of non-foamy macrophages and macrophage foam cells were observed. SMCs and elastic and collagen fibers were more sparsely distributed in the lipid core than in the lipid pool of PIT; however, the tissue structure was preserved. In addition, small, calcified foci were observed in the lesions.

ANC is defined as a lesion with a necrotic core composed of a lipid core-like region and liponecrotic tissue [9, 29, 30]. The infiltrations of non-foamy macrophages and macrophage foam cells were generally greater than those in PIT and ALC. The morphology of the lipid-core-like region of ANC was similar to that of the lipid core of ALC. The liponecrotic tissue consisted of

amorphous materials with abundant cholesterol clefts and lacked cells and connective tissue fibers. Moreover, calcification was observed.

Antibodies and reagents

The antibodies and reagents used in this study are listed in Additional Tables 2–5 [see Additional file 1].

Histologic examinations

Coronary arteries were fixed in 4% paraformaldehyde or 10% formalin and incised perpendicular to the long axis of the artery. Nineteen paraffin-embedded specimens containing typical PIT, ALC, or ANC lesions were obtained from 16 patients. One specimen was obtained from either the LAD or the RCA in 13 patients and two specimens were obtained from both the LAD and the RCA in three patients. Subsequently, the specimens were serially incised into 3 μm-thick sections. The basic structure of the artery was observed using H & E staining. EVG and PSR staining was used to observe the elastic and collagen fibers, respectively. The polarized light images of PSR-stained sections showed the distribution of collagen fibers. The internal elastic lamina was used for detection of the boundary between the intima and media. Whole-slide images of the stained sections, immunostained sections, and sections stained with CHP were created using a virtual slide scanner (NanoZoomer-XR, Hamamatsu Photonics, Hamamatsu City, Japan).

Immunohistochemistry and CHP staining

For immunohistochemistry, the sections were pretreated by autoclaving or Immunosaver treatment (Additional Table 2 [see Additional file 1]) and subsequently incubated with primary antibodies overnight at 4 °C. HistoGreen or 3,3'-diaminobenzidine tetrahydrochloride (DAB) was used as the substrate. Macrophages were identified through immunohistochemistry using an anti-CD68 antibody. SMCs were identified using an antibody cocktail against actin composed of anti-α-smooth muscle actin antibody and anti-human muscle actin antibody. The distribution of apoB, fibrinogen, collagen type I, collagen type III, elastin, CTX-I, and CatK was observed through immunohistochemistry using the respective antibodies. Non-immune mouse, rabbit, and goat immunoglobulin Gs were used as negative controls. Denatured and unfolded collagen chains were detected by CHP staining. Briefly, the biotin-conjugated CHP solution (20 μM) was heated at 80 °C for 5 min. After quenching, the solution was applied to de-paraffinized sections overnight. The sections were incubated with horseradish peroxidase-conjugated streptavidin, and the reaction products were visualized using DAB.

Double-immunohistochemistry was performed to investigate the relationship between the spatial distribution of macrophages and CatK. First, a section of the artery was immunostained with an anti-CD68 antibody using HistoGreen as the substrate and an image of the section was obtained using a virtual slide system. After removing the HistoGreen and anti-CD68 antibodies by Immunosaver treatment, the sections were immunostained with anti-CatK antibody using DAB as the substrate, and an image of the section was obtained again using a virtual slide system. Then, the distribution of macrophages and CatK was compared between the two images. The same method was used to investigate the relationship between the spatial distribution of SMCs and CatK.

Assessment of immunohistochemistry and CHP staining

The grade of staining for collagen type I, collagen type III, CTX-I, CatK, elastin, and CHP was assessed in PIT, ALC, the lipid core-like region of ANC, and the liponecrotic tissue of ANC. The number of arterial specimens examined was six, six, seven, and seven, respectively. Grades were scored from 0 to 3 according to the intensity and area of staining, with Grade 0: no staining; Grade 1: mild staining or moderate and focal staining; Grade 2: moderate and diffuse staining or intense and focal staining; Grade 3: intense and diffuse staining. The data are presented as scatter plots with medians. Furthermore, a radar chart was created using the median score of each substance to show the differences in the distribution of

the six substances among PIT, ALC, the lipid core-like region of ANC, and the liponecrotic tissue of ANC. The relationship between CTX-I and CatK was examined by comparing the grade of staining for both molecules and presented as a correlation chart. In this analysis, the data in PIT, ALC, the lipid core-like region of ANC, and the liponecrotic tissue of ANC were combined, with a total number of 26 examined arterial specimens.

Results

Morphology of PIT, ALC, and ANC

Six, six, and seven arteries were classified as PIT, ALC, and ANC, respectively. Figure 1 shows the representative histology of the three lesions. PIT showed a mildly thickened intima with lipid pools in the middle-to-lower layers of the intima. The lipid pools showed as lightly stained areas with EGV and PSR staining and loosely arranged collagen fibers in the polarized image of the PSR staining (Fig. 1a–c). In addition, the lesion was characterized by the accumulation of apoB, suggesting the infiltration and deposition of plasma-derived apoB-containing lipoproteins, such as low-density lipoproteins (Fig. 1d). This was supported by a positive immunostaining for another plasma-derived protein, fibrinogen (Additional Fig. 1a [see Additional file 1]). A small number of macrophages were observed in the superficial layer of the intima and SMCs were discretely distributed in the lipid pool (Fig. 1e–f). Similar morphological features were observed in ALC; however, the size of the lipid core was larger than that of the

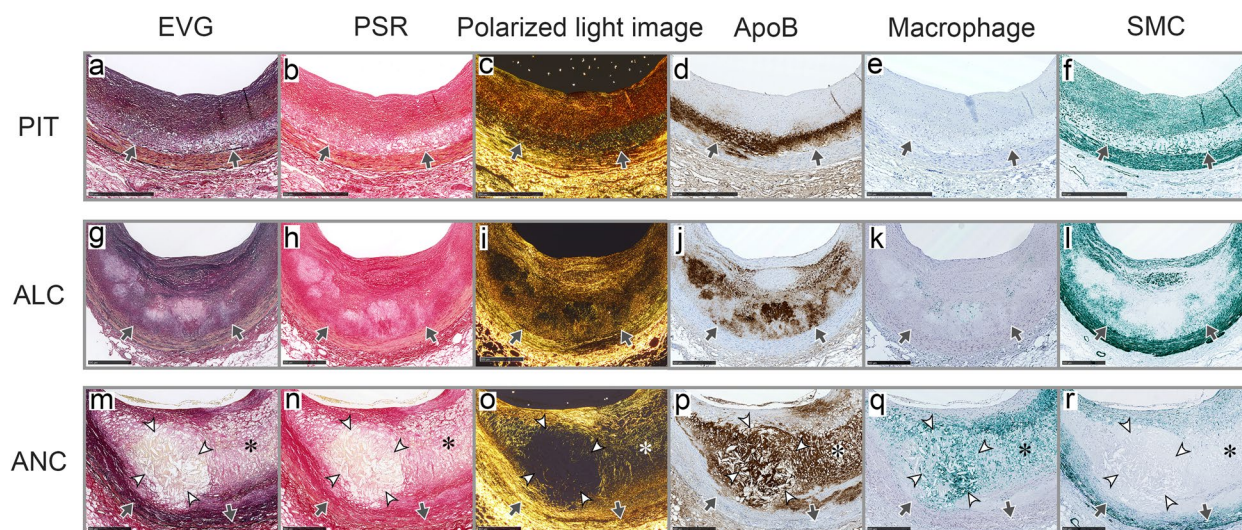


Fig. 1 Representative histology of the pathologic intimal thickening (PIT), atheroma with lipid core (ALC), and atheroma with necrotic core (ANC). **a–f** PIT. **g–l** ALC. **m–r** ANC. **a, g, m** Elastica van Gieson (EVG) staining. **b, h, n** Picrosirius red (PSR) staining. **c, i, o** Polarized light image of PSR-stained section. **d, j, p** Immunohistochemistry for apolipoprotein B (apoB). **e, k, q** Immunohistochemistry for CD68. **f, l, r** Immunohistochemistry for smooth muscle cells (SMCs). An asterisk and white arrowheads in ANC indicate a lipid core-like region and liponecrotic tissue, respectively (**m–r**). Black arrows indicate internal elastic lamina (**a–r**). Bars represent 500 μ m (**a–r**)

lipid pool in PIT (Fig. 1g-l). ApoB and fibrinogen were deposited in the lipid core (Fig. 1j, Additional Fig. 1b [see Additional file 1]), where elastic and collagen fibers and SMCs were discretely distributed (Fig. 1g-i, 1l), and a small number of macrophages were infiltrated (Fig. 1k). However, the tissue structure was preserved and no liponecrotic tissue developed in the lesion.

ANC consisted of a lipid core-like region and liponecrotic tissue (Fig. 1m-r and Additional Fig. 1c [see Additional file 1]). The lipid core-like region exhibited features similar to those of the lipid core of ALC and the tissue architecture was preserved. The liponecrotic tissue showed fully different features, consisting of amorphous materials with no or very few elastic and collagen fibers (Fig. 1m-n). The polarized light images of the PSR-stained sections showed a characteristic empty hole-like appearance due to the absence of collagen fibers (Fig. 1o). ApoB staining was diffusely positive in the ANC lesions, suggesting that the infiltration and deposition of apoB-containing lipoproteins occurred not only in the lipid core-like region but also in the liponecrotic tissue (Fig. 1p). The diffuse immunostaining for fibrinogen in the ANC lesions supports this suggestion (Additional Fig. 1c [see Additional file 1]). A large number of macrophages were observed within and around the liponecrotic tissue (Fig. 1q), and SMCs were found to be few in the lipid core-like region and absent in the liponecrotic tissue (Fig. 1r).

Localization of connective tissue fibers and related substances

Figure 2 shows representative immunohistochemical and histological images demonstrating the localization of collagen type I, denatured and unfolded collagen chains detected by CHP staining, elastin, collagen type III, CTX-I, and CatK in PIT, ALC, and ANC. All six substances generally demonstrated diffuse or patchy staining patterns in PIT (Fig. 2a-f), ALC (Fig. 2g-l), and the lipid core-like region of ANC (Fig. 2m-r), although the staining intensity varied between the arteries. In contrast, the liponecrotic tissue of ANC (Fig. 2m-r) showed negative staining for collagen type I, denatured and unfolded collagen chains, and elastin (Fig. 2m-o), but moderate-to-intense staining for collagen type III, CTX-I, and CatK (Fig. 2p-r).

Grade of immunostaining and CHP staining

Figure 3a-d shows the staining grades of collagen type I, CHP staining, elastin, collagen type III, CTX-I, and CatK in PIT, ALC, the lipid core-like region of ANC, and the liponecrotic tissue of ANC. The grades for each arterial specimen are presented as plots in the figures. PIT, ALC, and the lipid core-like region of ANC generally demonstrated similar patterns, as the grade of staining for collagen type I, CHP, and elastin was relatively high, whereas that for CTX-I and CatK was relatively low (Fig. 3a-c). However, the liponecrotic tissue of ANC showed the opposite pattern, and all arterial specimens showed

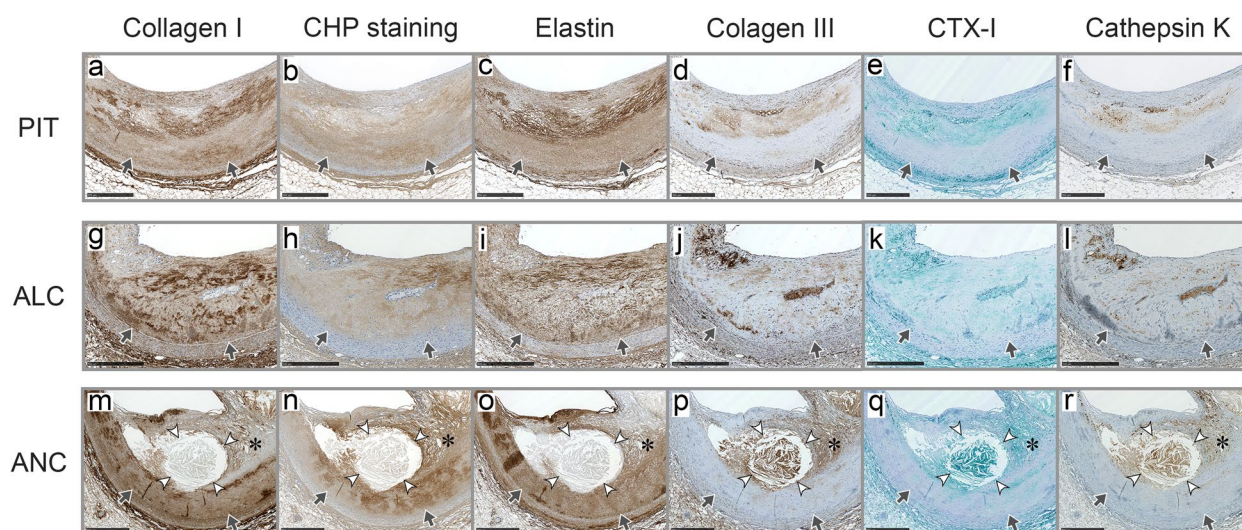


Fig. 2 Localization of collagen type I (Collagen I), denatured and unfolded collagen chains detected by collagen hybridizing peptide (CHP) staining, elastin, collagen type III (Collagen III), C-terminal crosslinked telopeptide of collagen type I (CTX-I), and cathepsin K (CatK) in the pathologic intimal thickening (PIT), atheroma with lipid core (ALC), and atheroma with necrotic core (ANC). **a-f** PIT. **g-l** ALC. **m-r** ANC. **a, g, m** Immunohistochemistry for collagen type I. **b, h, n** CHP staining. **c, i, o** Immunohistochemistry for elastin. **d, j, p** Immunohistochemistry for collagen type III. **e, k, q** Immunohistochemistry for CTX-I. **f, l, r** Immunohistochemistry for CatK. An asterisk and white arrowheads in ANC indicate a lipid core-like region and liponecrotic tissue, respectively (**m-r**). Black arrows indicate internal elastic lamina (**a-r**). Bars represent 500 μ m (**a-r**)

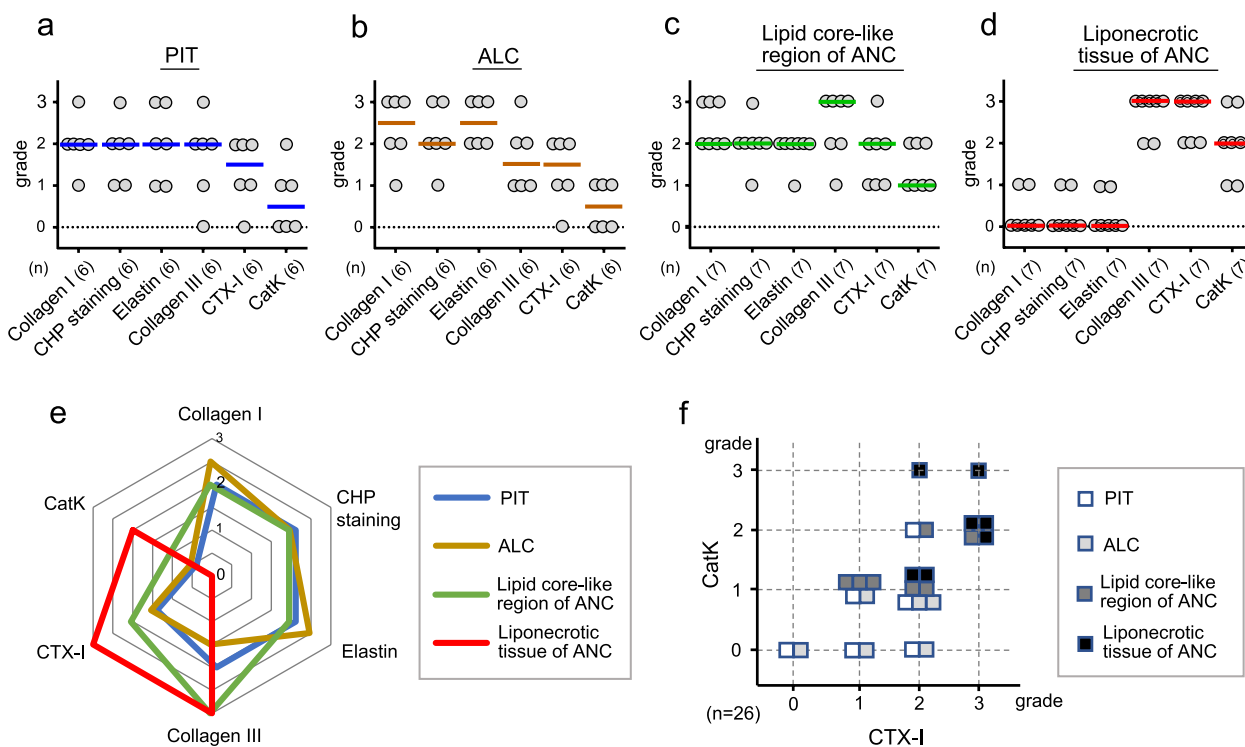


Fig. 3 Assessment of immunohistochemistry for collagen type I (Collagen I), elastin, collagen type III (Collagen III), C-terminal crosslinked telopeptide of collagen type I (CTX-I), and cathepsin K (CatK), and collagen hybridizing peptide (CHP) staining, in the pathologic intimal thickening (PIT), atheroma with lipid core (ALC), lipid core-like region of atheroma with necrotic core (ANC), and liponecrotic tissue of ANC. CHP staining detects denatured and unfolded collagen chains. **a–d** Staining grade for each substance in PIT (**a**), ALC (**b**), the lipid core-like region of ANC (**c**), and the liponecrotic tissue of ANC (**d**). Bars represent median scores (**a–d**). **e** Rader chart using the median score for each substance in PIT, ALC, lipid core-like region of ANC, and liponecrotic tissue of ANC. **f** Correlation chart between the grade of immunohistochemistry for CTX-I and CatK in PIT, ALC, the lipid core-like region of ANC, and the liponecrotic tissue of ANC. The numbers in parenthesis (n) indicate the number of specimens

Grade 0 or 1 for collagen type I, CHP staining, and elastin, whereas many specimens demonstrated higher grades (Grades 2 and 3) for CTX-I and CatK (Fig. 3d). The grade of collagen type III showed a specific pattern, being higher in the lipid core-like region and liponecrotic tissue of ANC than in PIT and ALC (Fig. 3a–d). The radar chart using the median of each substance shows the differences between the liponecrotic tissue of ANC and the other three regions (Fig. 3e). Figure 3f shows that a positive relationship between the grade of CTX-I and CatK staining appeared to be present. In particular, both CTX-I and CatK showed higher grades in liponecrotic tissue (Fig. 3f).

Cell species producing CatK

The double immunohistochemistry results revealed that CatK was moderately-to-intensely stained in macrophages (Fig. 4a–b), particularly in macrophage foam cells (Fig. 4c–d). Although the relationship between CatK and SMCs was not conspicuous in the low-power view (Fig. 4e–f), the high-power view revealed that CatK was weakly immunostained in the cytoplasm of SMCs

(Fig. 4g–h). These findings suggest that CatK is produced mainly by macrophages, especially macrophage foam cells, and mildly by SMCs.

Discussion

Characteristics of human atheroma

The pathogenesis of human atheroma remains unclear. A previous study involving the American Heart Association described the core of atheroma as a lipid core and suggested that infiltration of plasma lipids played an important role in core formation [3]. Meanwhile, another study by Virmani et al. referred to the core of atheroma as a necrotic core and described it as a lesion containing lipids with abundant cholesterol crystals and cellular debris [16, 29, 30]. Thus, the concept of atheroma differs among researchers, and the definitions of the lipid and necrotic cores are ambiguous. Our study suggested that atheromas are divided into ALC and ANC, and the lipid core and the necrotic core are appropriate terms for expressing the characteristics of ALC and ANC, respectively [9].

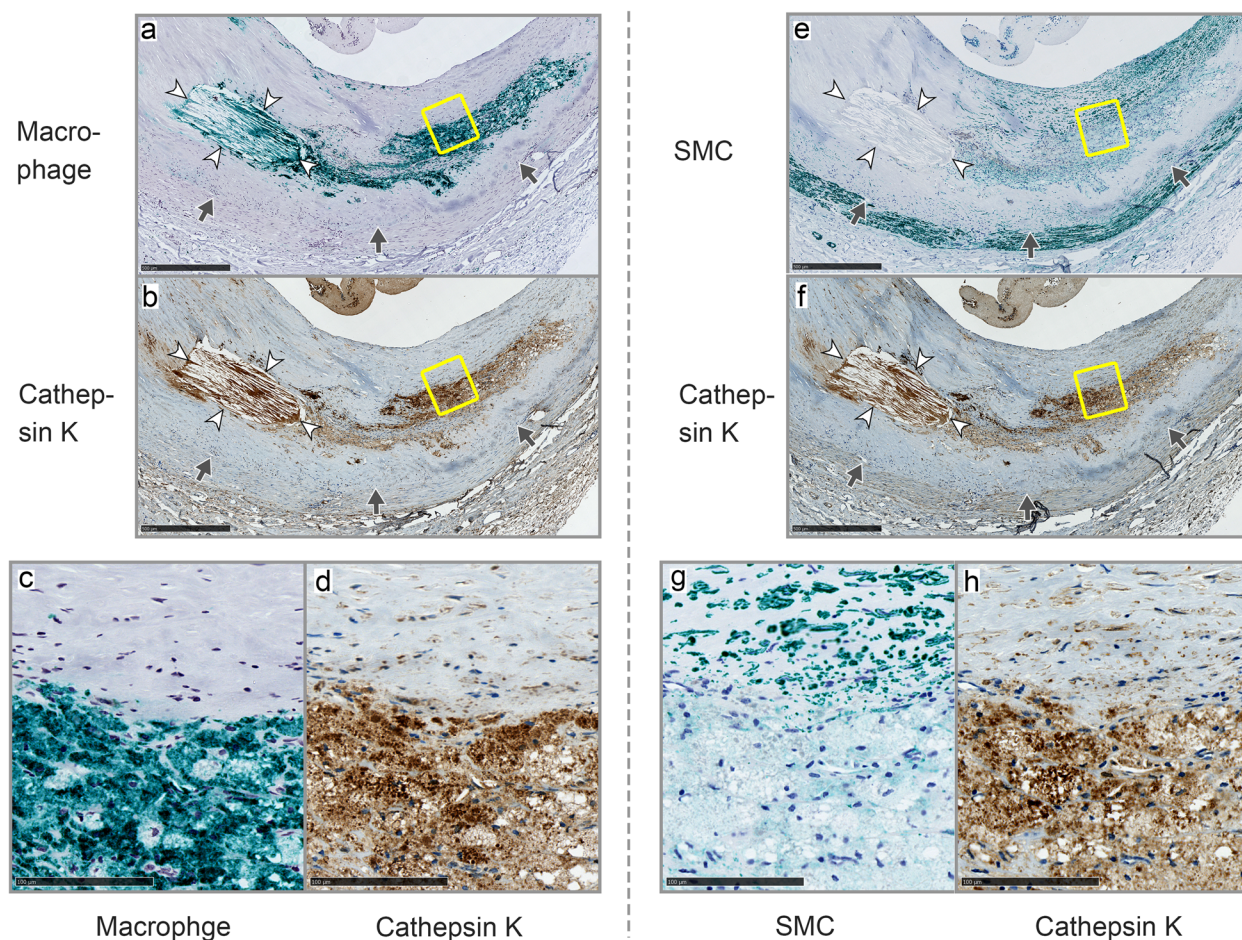


Fig. 4 Double immunohistochemistry of macrophages and cathepsin K (CatK) and smooth muscle cells (SMCs) and CatK. **a–d** Low- and high-power views of immunohistochemistry for CD68 (**a, c**) and CatK (**b, d**) in the same section of the atheroma with necrotic core (ANC). The figures in the panels **c** and **d** are taken from the rectangle region shown in the panels **a** and **b**, respectively. **e–h** Low- and high-power views of immunohistochemistry for SMCs (**e, g**) and CatK (**f, h**) in the same section of ANC. The figures in the panels **g** and **h** are taken from the rectangle region in the panels **e** and **f**, respectively. White arrowheads in the panels **a, b, e**, and **f** indicate liponecrotic tissue. Black arrows indicate internal elastic lamina (**a, b, e, f**). Bars represent 500 μm (**a, b, e, f**) and 100 μm (**c, d, g, h**)

The origin of lipid deposition in atherosclerotic lesions is still under debate. Our previous study using matrix-assisted laser desorption/ionization imaging mass spectrometry suggested that the lipids in the lipid pool of PIT, the lipid core of ALC, the lipid core-like region of ANC and, importantly, the liponecrotic tissue of ANC as well were mainly derived from the plasma [9]. This concept is further supported in this study by the presence of plasma-derived proteins, apoB and fibrinogen, in all four regions. However, PSR and EVG staining revealed a different feature in the liponecrotic tissue compared to the other three regions, indicating the absence of collagen and elastic fibers. One possible explanation for these findings is that pre-existing collagen and elastic fibers were degraded and lost in the liponecrotic tissue, whereas plasma-derived substances, including lipids, remained in this tissue.

Specificity of liponecrotic tissue

This study revealed specific features of liponecrotic tissues, including the absence of collagen type I, denatured and unfolded collagen chains, and elastin and the presence of CTX-I and CatK. Collagen type I belongs to the fibrillar collagen group and may contribute to maintaining the integrity of the tissue structure [19, 31]. Its absence in liponecrotic tissues supports the hypothesis that intact collagen fibers are degraded and lost, leading to the collapse of the tissue structure. Furthermore, the states of the denatured and unfolded collagen chains, CTX-I, and CatK provided important clues regarding how and to what extent the collagen fibers were degraded. Denatured and unfolded collagen chains were detected by CHP, which contains a repeating glycine-proline-hydroxyproline sequence that specifically binds to unfolded collagen chains [22]. In an animal model, partial

collagen damage detected by CHP staining was shown to be a hallmark of the early phase of atherosclerosis [32]. The present study demonstrated that CHP staining was positive in PIT, ALC, and the lipid core-like regions of ANC and negative in the liponecrotic tissue of ANC. These findings suggested that, in humans, the partial damage of collagen fibers continuously occurred even in intermediate and advanced lesions, and that collagen was more severely damaged in the liponecrotic tissue.

CTX-I is a fragmented peptide consisting of C-terminal region of collagen type I and generated by CatK [24, 25]. CatK possesses potent collagenolytic and elastinolytic activities and cleaves collagen type I at multiple sites [26]. In the human body, it is predominantly secreted by activated osteoclasts during bone resorption, which is reflected by an increase in CTX-I in the serum and urine [33, 34]. Meanwhile, CatK is also found in various organs and diseased sites including atherosclerotic lesions [33, 35, 36]. In this study, CTX-I and CatK were detected in intermediate and advanced lesions, with the staining grades appearing to correlate. In particular, these molecules were the most intensely stained in the liponecrotic tissue where collagen type I was absent. These findings suggest that type I collagen was severely degraded in the liponecrotic tissue of ANC by CatK, and that CTX-I was deposited in the region. Importantly, loss of connective tissue fibers in the liponecrotic tissue of ANC are closely related to plaque instability, and possibly rupture. Compatible findings were reported in double CatK and apolipoprotein E (CatK^{-/-}/ApoE^{-/-}) knockout mice by Lutgens et al., who demonstrated that a deficiency of CatK leads to a higher collagen content in atherosclerotic lesions and increases plaque stability [35].

Elastin was not immunostained in the liponecrotic tissue. This observation was consistent with the absence of elastic fibers in EVG staining and supported the hypothesis of connective tissue loss in the region. Collagen type III showed positive immunostaining in the liponecrotic tissue. However, no intact collagen fibers were present in this region because no PSR staining was observed. Collagen type III is cleaved by matrix metalloproteinases (MMPs) at a single site [37]; therefore, the immunoreactive site may have remained within the cleaved molecule.

Production of CatK by macrophages

This study suggests that CatK is mainly produced by macrophages, particularly macrophage foam cells, although SMCs also contain this enzyme in their cytoplasm. However, because CatK is a lysosomal enzyme, ordinary immunohistochemistry cannot distinguish between active CatK and its precursors, which lack proteolytic activity. Using a protease-activatable fluorescence sensor, Jaffer et al. revealed the preferential localization of

enzymatically active CatK in macrophages rather than in SMCs [36]. As shown in our study, a high number of macrophage foam cells infiltrated ANC, particularly in and around the liponecrotic tissue [9], suggesting that macrophage foam cells actively participate in degrading connective tissue fibers by secreting active CatK. Similarly, Barascuk et al. found that human monocytes cultured on a collagen type I-enriched matrix produced CTX-I, with a CatK inhibitor reducing CTX-I production [38].

Understanding how the production of CatK is stimulated and how its activation is promoted is of special importance. Interestingly, monocyte-related and CatK-positive osteoclast-like cells are present in atherosclerotic lesions and are closely associated with calcification [39]. These osteoclast-like cells, together with CatK-positive macrophages, may be involved in degrading calcified deposits, similarly to how genuine osteoclasts degrade bone tissue. However, Chinetti-Gbaguidi et al. demonstrated that macrophages surrounding calcium deposits in atherosclerotic plaques are characterized by low CatK expression and activity, suggesting a defective calcification resorption ability [40]. Thus, these findings suggest that the production and activation of CatK in atherosclerotic lesions are stimulated by calcification, but CatK may not be effective enough to remove all the calcified deposits. This is an important possible explanation for the pathogenesis of calcified lesions in humans. However, another crucial point is the inflammatory effect of this enzyme on tissues other than calcium deposits. CatK secreted by macrophages into the extracellular space may concomitantly degrade connective tissue fibers and consequently contribute to the formation of the liponecrotic tissue. Meanwhile, it is worth noting that the expression of CatK is induced *in vitro* by factors other than calcification, such as hypoxia and vascular endothelial growth factor (VEGF) [41]. In fact, the atherosclerotic lesions are hypoxic *in vivo* and VEGF is localized in human lesions [42, 43], suggesting that these factors may also contribute to the degradation of connective tissue fibers by producing CatK. Lutgens et al. also reported that oxidized LDL uptake by bone marrow-derived macrophages was increased in double CatK and apolipoprotein E knockout mice and suggested that CatK deficiency aggravates foam cell formation [35]. In addition, they suggested that caveolins and CD36 play important roles in this uptake mechanism [44].

Limitations

This study has some limitations. First, the sample number was small, and as such this is a pilot study, but we believe that our results provide a novel concept and useful indications. In this study, we used CD68 and actins to

identify macrophage and SMCs, respectively. However, it is known that phenotypically altered SMCs showing an immunopositive reaction for both CD68 and α -smooth muscle actin are present in human atherosclerotic lesions [45]. Thus, it is possible that these phenotypically altered macrophage-like SMCs secrete high levels of CatK. To investigate the production of CatK by these phenotypically altered cells, more detailed analysis is necessary. In addition, being based on immunohistochemical findings, we hypothesized that macrophage foam cells are a predominant source of CatK. To substantiate this hypothesis, further studies are warranted to quantify the relative expression of CatK in human peripheral blood mononuclear cells and SMC cell lines upon lipid loading.

Conclusions

We have been studying the pathogenesis of human atherosclerosis from the early to advanced stages [6–9]. One of the most important suggestions obtained from our former and present studies is that human atherosclerosis is mainly caused in two steps. The first step is based on quantitative changes [7–9]. The size of the lesion increases from the early to advanced stages, a phenomenon accompanied by the accumulation of plasma-derived lipids. The second step is based on qualitative changes, as shown in the previous [9] and present studies. A part of the lipid core of atheroma is transformed into the liponecrotic tissue of the necrotic core through degradation of connective tissue fibers and collapse of the tissue structure, accompanied by macrophage infiltration. Importantly, this study suggests that the inflammatory reactions involving macrophage-secreted CatK may play an important role in the degradation process. Meanwhile, other proteolytic enzymes, such as MMPs, also appear to be involved in the cleavage of connective tissue fibers in atherosclerotic lesions [46, 47]. Our previous study showed that MMP-1 and MMP-9 are localized in macrophages that infiltrate around the liponecrotic tissue [9]. Future studies are warranted to fully elucidate the role of proteolytic enzymes, including CatK, in the degradation of connective tissue fibers and formation of liponecrotic tissue in ANC. Furthermore, biochemical studies are necessary to characterize the degradation products of collagen and elastic fibers in the liponecrotic tissue. Such better understanding could help develop an effective way to prevent progression of atherosclerosis and plaque rupture in the future.

Abbreviations

WHO	World Health Organization
CVD	Cardiovascular disease
IHD	Ischemic heart disease
PIT	Pathologic intimal thickening
ALC	Atheroma with lipid core
ANC	Atheroma with necrotic core

CTX-I	C-terminal crosslinked telopeptide of collagen type I
CatK	Cathepsin K
CHP	Collagen hybridizing peptide
LAD	Left anterior descending artery
RCA	Right coronary artery
H & E	Hematoxylin and eosin
EVG	Elastica van Gieson
PSR	Picrosirius red
apoB	Apolipoprotein B
SMC	Smooth muscle cell
DAB	3,3'-Diaminobenzidine tetrahydrochloride
MMP	Matrix metalloproteinase
VEGF	Vascular endothelial growth factor
Collagen I	Collagen type I
Collagen III	Collagen type III

Supplementary Information

The online version contains supplementary material available at <https://doi.org/10.1186/s41231-024-00188-6>.

Additional file 1: Additional Table 1 Principal disease of autopsy patients. Additional Table 2 Primary antibodies. Additional Table 3 Collagen hybridizing peptide, immunohistochemistry kit, secondary antibody, and streptavidin. Additional Table 4 Non-immune immunoglobulins. Additional Table 5 Substrates for immunohistochemistry and collagen hybridizing peptide staining. Additional Fig. 1 Immunohistochemical localization of fibrinogen in the PIT, ALC and ANC.

Acknowledgements

We would like to thank Yong-Xiang Chen of the Department of Cardiac Sciences, University of Calgary, Calgary, Alberta, Canada for collecting the coronary artery specimens and Hiroshi Fujii of the Pathophysiological and Experimental Pathology, Graduate School of Medical Sciences, Kyushu University, Fukuoka, Japan for the excellent technical assistance. We would also like to thank Editage (www.editage.com) for the English language editing.

Authors' contributions

KN and YN collaborated to design the study; collect, analyze, and interpret the data; and write the manuscript. All authors read and approved the final manuscript.

Funding

This study was supported by a Grant-in-Aid for Scientific Research from the Japan Society for the Promotion of Science (grant number JP26670177, KN).

Availability of data and materials

The data that support the findings of the study are available from the corresponding author upon reasonable request.

Declarations

Ethics approval and consent to participate

This study was approved by the Kyushu University Certified Institutional Review Board for Clinical Trials (approval no. 29–339) and was performed in accordance with the institutional guidelines.

Consent for publication

Not applicable.

Competing interests

The authors declare that they have no competing interests.

Received: 1 April 2024 Accepted: 25 August 2024

Published online: 04 September 2024

References

1. WHO/Newsroom/Fact sheets/Detail/Cardiovascular diseases (CVDs). <https://www.who.int/news-room/fact-sheets/detail/cardiovascular-diseases-cvds>. Accessed 14 Jul 2024.
2. Stary HC, Chandler AB, Glagov S, Guyton JR, Insull W Jr, Rosenfeld ME, Schaffer SA, Schwartz CJ, Wagner WD, Wissler RW. A definition of initial, fatty streak, and intermediate lesions of atherosclerosis. A report from the Committee on Vascular Lesions of the Council on Arteriosclerosis, American Heart Association. *Circulation*. 1994;89:2462–78. <https://doi.org/10.1161/01.cir.89.5.2462>.
3. Stary HC, Chandler AB, Dinsmore RE, Fuster V, Glagov S, Insull W Jr, Rosenfeld ME, Schwartz CJ, Wagner WD, Wissler RW. A definition of advanced types of atherosclerotic lesions and a histological classification of atherosclerosis. A report from the Committee on Vascular Lesions of the Council on Arteriosclerosis, American Heart Association. *Circulation*. 1995;92:1355–74. <https://doi.org/10.1161/01.cir.92.5.1355>.
4. Virmani R, Kolodgie FD, Burke AP, Farb A, Schwartz SM. Lessons from sudden coronary death. A comprehensive morphological classification scheme for atherosclerotic lesions. *Arterioscler Thromb Vasc Biol*. 2000;20:1262–75. <https://doi.org/10.1161/01.ATV.20.5.1262>.
5. Kawai K, Kawakami R, Finn AV, Virmani R. Differences in stable and unstable atherosclerotic plaque. *Arterioscler Thromb Vasc Biol*. 2024;44:1474–84. <https://doi.org/10.1161/ATVBAHA.124.319396>.
6. Nakashima Y, Chen YX, Kinukawa N, Sueishi K. Distributions of diffuse intimal thickening in human arteries: preferential expression in atherosclerosis-prone arteries from an early age. *Virchows Arch*. 2002;441:279–88. <https://doi.org/10.1007/s00428-002-0605-1>.
7. Nakashima Y, Fujii H, Sumiyoshi S, Wight TN, Sueishi K. Early human atherosclerosis. Accumulation of lipid and proteoglycans in intimal thickenings followed by macrophage infiltration. *Arterioscler Thromb Vasc Biol*. 2007;27:1159–65. <https://doi.org/10.1161/ATVBAHA.106.134080>.
8. Nakagawa K, Nakashima Y. Pathologic intimal thickening in human atherosclerosis is formed by extracellular accumulation of plasma-derived lipids and dispersion of intimal smooth muscle cells. *Atherosclerosis*. 2018;274:235–42. <https://doi.org/10.1016/j.atherosclerosis.2018.03.039>.
9. Nakagawa K, Tanaka M, Hahm TH, Nguyen HN, Matsui T, Chen YX, Nakashima Y. Accumulation of plasma-derived lipids in the lipid core and necrotic core of human atheroma: imaging mass spectrometry and histopathological analyses. *Arterioscler Thromb Vasc Biol*. 2021;41:e498–511. <https://doi.org/10.1161/ATVBAHA.121.316154>.
10. Getz GS, Reardon CA. Animal models of atherosclerosis. *Arterioscler Thromb Vasc Biol*. 2012;32:1104–15. <https://doi.org/10.1161/ATVBAHA.111.237693>.
11. Nakashima Y, Plump AS, Raines EW, Breslow JL, Ross R. ApoE-deficient mice develop lesions of all phases of atherosclerosis throughout the arterial tree. *Arterioscler Thromb*. 1994;14:133–40. <https://doi.org/10.1161/01.ATV.14.1.133>.
12. Ishibashi S, Brown MS, Goldstein JL, Gerard RD, Hammer RE, Herz J. Hypercholesterolemia in low density lipoprotein receptor knockout mice and its reversal by adenovirus-mediated gene delivery. *J Clin Invest*. 1993;92:883–93. <https://doi.org/10.1172/JCI116663>.
13. Watanabe Y. Serial inbreeding of rabbits with hereditary hyperlipidemia (WHHL-RABBIT). *Atherosclerosis*. 1980;36:261–8. [https://doi.org/10.1016/0021-9150\(80\)90234-8](https://doi.org/10.1016/0021-9150(80)90234-8).
14. Bentzon JF, Otsuka F, Virmani R, Falk E. Mechanisms of plaque formation and rupture. *Circ Res*. 2014;114:1852–66. <https://doi.org/10.1161/CIRCRESAHA.114.302721>.
15. Cullen P, Baetta R, Bellosta S, Bernini F, Chinetti G, Cignarella A, von Eckardstein A, Exley A, Goddard M, Hofker M, Hurt-Camajó E, Kanters E, Kovanen P, Lorkowski S, McPheat W, Pentikäinen M, Rauterberg J, Ritchie A, Staels B, Weitekamp B, de Winther M, for the MAFAPS Consortium. Rupture of the atherosclerotic plaque. Does a good animal model exist? *Arterioscler Thromb Vasc Biol*. 2003;23:535–42. <https://doi.org/10.1161/01.ATV.0000060200.73623.F8>.
16. Yahagi K, Kolodgie FD, Otsuka F, Finn AV, Davis HR, Joner M, Virmani R. Pathophysiology of native coronary, vein graft, and in-stent atherosclerosis. *Nat Rev Cardiol*. 2016;13:79–98. <https://doi.org/10.1038/nrcardio.2015.164>.
17. Nakashima Y, Kiyohara Y, Doi Y, Kubo M, Iida M, Sueishi K. Risk factors for coronary atherosclerosis in a general Japanese population: the Hisayama study. *Pathol Res Pract*. 2009;205:700–8. <https://doi.org/10.1016/j.prp.2009.05.002>.
18. Seimon T, Tabas I. Mechanisms and consequences of macrophage apoptosis in atherosclerosis. *J Lipid Res*. 2009;50(Suppl):S382–7. <https://doi.org/10.1194/jlr.R800032-JLR200>.
19. Katsuda S, Okada Y, Minamoto T, Oda Y, Matsui Y, Nakanishi I. Collagens in human atherosclerosis. Immunohistochemical analysis using collagen type-specific antibodies. *Arterioscler Thromb*. 1992;12:494–502. <https://doi.org/10.1161/01.ATV.12.4.494>.
20. Barnes MJ, Farndale RW. Collagens and atherosclerosis. *Exp Gerontol*. 1999;34:513–25. [https://doi.org/10.1016/s0531-5565\(99\)00038-8](https://doi.org/10.1016/s0531-5565(99)00038-8).
21. Cociolone AJ, Hawes JZ, Staiculescu MC, Johnson EO, Murshed M, Wagenseil JE. Elastin, arterial mechanics, and cardiovascular disease. *Am J Physiol Heart Circ Physiol*. 2018;315:H189–205. <https://doi.org/10.1152/ajpheart.00087.2018>.
22. Hwang J, Huang Y, Burwell TJ, Peterson NC, Connor J, Weiss SJ, Yu SM, Li Y. In situ imaging of tissue remodeling with collagen hybridizing peptides. *ACS Nano*. 2017;11:9825–35. <https://doi.org/10.1021/acsnano.7b03150>.
23. Li Y, Yu SM. In situ detection of degraded and denatured collagen via triple helical hybridization: new tool in histopathology. *Methods Mol Biol*. 2019;1944:135–44. https://doi.org/10.1007/978-1-4939-9095-5_10.
24. Herrmann M, Seibel M. The amino- and carboxyterminal cross-linked telopeptides of collagen type I, NTX-I and CTX-I: a comparative review. *Clin Chim Acta*. 2008;393:57–75. <https://doi.org/10.1016/j.cca.2008.03.020>.
25. Garnero P, Ferreras M, Karsdal MA, Nicamhlaibh R, Risteli J, Borel O, Qvist P, Delmas PD, Foged NT, Delaïssé JM. The type I collagen fragments ICTP and CTX reveal distinct enzymatic pathways of bone collagen degradation. *J Bone Miner Res*. 2003;18:859–67. <https://doi.org/10.1359/jbmr.2003.18.5.859>.
26. Garnero P, Borel O, Byrjalsen I, Ferreras M, Drake FH, McQueney MS, Foged NT, Delmas PD, Delaïssé JM. The collagenolytic activity of cathepsin K is unique among mammalian proteinases. *J Biol Chem*. 1998;273:32347–52. <https://doi.org/10.1074/jbc.273.48.32347>.
27. Sukhova GK, Shi GP, Simon DI, Chapman HA, Libby P. Expression of the elastolytic cathepsins S and K in human atheroma and regulation of their production in smooth muscle cells. *J Clin Invest*. 1998;102:576–83. <https://doi.org/10.1172/JCI181>.
28. Ogawa W, Hirota Y, Miyazaki S, Nakamura T, Ogawa Y, Shimomura I, Yamauchi T, Yokote K, Creation Committee for Guidelines for the Management of Obesity Disease 2022 by Japan Society for the Study of Obesity (JASSO). Definition, criteria, and core concepts of guidelines for the management of obesity disease in Japan. *Endocr J*. 2024;71:223–31. <https://doi.org/10.1507/endocrj.EJ23-0593>.
29. Otsuka F, Kramer MC, Woudstra P, Yahagi K, Ladich E, Finn AV, de Winter RJ, Kolodgie FD, Wight TN, Davis HR, Joner M, Virmani R. Natural progression of atherosclerosis from pathologic intimal thickening to late fibroatheroma in human coronary arteries: a pathology study. *Atherosclerosis*. 2015;241:772–82. <https://doi.org/10.1016/j.atherosclerosis.2015.05.011>.
30. Sakakura K, Nakano M, Otsuka F, Ladich E, Kolodgie FD, Virmani R. Pathophysiology of atherosclerosis plaque progression. *Heart Lung Circ*. 2013;22:399–411. <https://doi.org/10.1016/j.hlc.2013.03.001>.
31. Wittig C, Szulcek R. Extracellular matrix protein ratios in the human heart and vessels: how to distinguish pathological from physiological changes? *Front Physiol*. 2021;12:708656. <https://doi.org/10.3389/fphys.2021.708656>.
32. Smith KA, Lin AH, Stevens AH, Yu SM, Weiss JA, Timmins LH. Collagen molecular damage is a hallmark of early atherosclerosis development. *J Cardiovasc Transl Res*. 2023;16:463–72. <https://doi.org/10.1007/s12265-022-10316-y>.
33. Dai R, Wu Z, Chu HY, Lu J, Lyu A, Liu J, Zhang G. Cathepsin K: The action in and beyond bone. *Front Cell Dev Biol*. 2020;8:433. <https://doi.org/10.3389/fcell.2020.00433>.
34. Kawana K, Takahashi M, Hoshino H, Kushida K. Comparison of serum and urinary C-terminal telopeptide of type I collagen in aging, menopause and osteoporosis. *Clin Chim Acta*. 2002;316:109–15. [https://doi.org/10.1016/s0009-8981\(01\)00742-2](https://doi.org/10.1016/s0009-8981(01)00742-2).
35. Lutgens E, Lutgens SPM, Faber BCG, Heeneman S, Gijbels MMJ, de Winther MPJ, Frederik P, van der Made I, Daugherty A, Sijbers AM, Fisher A, Long CJ, Saftig P, Black D, Daemen MJAP, Cleutjens KBJM. Disruption of the cathepsin K gene reduces atherosclerosis progression and induces

- plaque fibrosis but accelerates macrophage foam cell formation. *Circulation*. 2006;113:98–107. <https://doi.org/10.1161/CIRCULATIONAHA.105.561449>.
36. Jaffer FA, Kim DE, Quinti L, Tung CH, Aikawa E, Pande AN, Kohler RH, Shi GP, Libby P, Weissleder R. Optical visualization of cathepsin K activity in atherosclerosis with a novel, protease-activatable fluorescence sensor. *Circulation*. 2007;115:2292–8. <https://doi.org/10.1161/CIRCULATIONAHA.106.660340>.
 37. Fields GB. Interstitial collagen catabolism. *J Biol Chem*. 2013;288:8785–93. <https://doi.org/10.1074/jbc.R113.451211>.
 38. Barascuk N, Skjöt-Arkil H, Register TC, Larsen L, Byrjalsen I, Christiansen C, Karsdal MA. Human macrophage foam cells degrade atherosclerotic plaques through cathepsin K mediated processes. *BMC Cardiovasc Disord*. 2010;10:19. <https://doi.org/10.1186/1471-2261-10-19>.
 39. Qiao JH, Mishra V, Fishbein MC, Sinha SK, Rajavashisth TB. Multinucleated giant cells in atherosclerotic plaques of human carotid arteries: identification of osteoclast-like cells and their specific proteins in artery wall. *Exp Mol Pathol*. 2015;99:654–62. <https://doi.org/10.1016/j.yexmp.2015.11.010>.
 40. Chinetti-Gbaguidi G, Daoudi M, Rosa M, Vinod M, Louvet L, Copin C, Fanchon M, Vanhoutte J, Derudas B, Belloy L, Haulon S, Zawadzki C, Susen S, Massy ZA, Eeckhoutte J, Staels B. Human alternative macrophages populate calcified areas of atherosclerotic lesions and display impaired RANKL-induced osteoclastic bone resorption activity. *Circ Res*. 2017;121:19–30. <https://doi.org/10.1161/CIRCRESAHA.116.310262>.
 41. Jiang H, Cheng XW, Shi GP, Hu L, Inoue A, Yamamura Y, Wu H, Takeshita K, Li X, Huang Z, Song H, Asai M, Hao CN, Unno K, Koike T, Oshida Y, Okumura K, Murohara T, Kuzuya M. Cathepsin K-mediated notch1 activation contributes to neovascularization in response to hypoxia. *Nat Commun*. 2014;5:3838. <https://doi.org/10.1038/ncomms4838>.
 42. Björnheden T, Levin M, Evaldsson M, Wiklund O. Evidence of hypoxic areas within the arterial wall in vivo. *Arterioscler Thromb Vasc Biol*. 1999;19:870–6. <https://doi.org/10.1161/01.atv.19.4.870>.
 43. Chen YX, Nakashima Y, Tanaka K, Shiraishi S, Nakagawa K, Sueishi K. Immunohistochemical expression of vascular endothelial growth factor/vascular permeability factor in atherosclerotic intimas of human coronary arteries. *Arterioscler Thromb Vasc Biol*. 1999;19:131–9. <https://doi.org/10.1161/01.ATV.19.1.131>.
 44. Lutgens SPM, Kisters N, Lutgens E, van Haften RIM, Evelo CTA, de Winther MPJ, Saftig P, Daemen MJAP, Heeneman S, Cleutjens KBJM. Gene profiling of cathepsin K deficiency in atherogenesis: profibrotic but lipogenic. *J Pathol*. 2006;210:334–43. <https://doi.org/10.1002/path.2054>.
 45. Allahverdian S, Chehroudi AC, McManus BM, Abraham T, Francis GA. Contribution of intimal smooth muscle cells to cholesterol accumulation and macrophage-like cells in human atherosclerosis. 2014;129:1551–9. <https://doi.org/10.1161/CIRCULATIONAHA.113.005015>.
 46. Galis ZS, Sukhova GK, Lark MW, Libby P. Increased expression of matrix metalloproteinases and matrix degrading activity in vulnerable regions of human atherosclerotic plaques. *J Clin Invest*. 1994;94:2493–503. <https://doi.org/10.1172/JCI117619>.
 47. Gough PJ, Gomez IG, Wille PT, Raines EW. Macrophage expression of active MMP-9 induces acute plaque disruption in apoE-deficient mice. *J Clin Invest*. 2006;116:59–69. <https://doi.org/10.1172/JCI25074>.

Publisher's Note

Springer Nature remains neutral with regard to jurisdictional claims in published maps and institutional affiliations.